

Wavelet Functional Data Analysis for FANOVA Models under Dependent Errors

Airton Kist ⁽¹⁾, Aluísio Pinheiro^{(2)*}

⁽¹⁾ University of Ponta Grossa, Brazil, ⁽²⁾ University of Campinas, Brazil

Abstract

We extend the wavelet tests for fixed effects FANOVA models with iid errors, proposed in Abramovich et al, 2004 to FANOVA models with dependent errors and provide an iterative Cochrane-Orcutt type procedure to estimate the parameters and the functional. The function is estimated through a nonlinear wavelet estimator. Nonparametric tests based on the optimal performance of nonlinear wavelet estimators are also proposed. The method is illustrated on real data sets and in simulated studies. The simulation also addresses the test performance under realistic sample sizes.

Keywords: Cochrane-Orcutt; Functional Data Analysis; Nonparametric Test; Nonparametric Inference.

MSC2000: primary-62G10; secondary-62G20;

1 The model

Consider the Ornstein-Uhlenbeck diffusion process as follows:

$$dy(t) = \rho_c y(t) dt + \sigma dW(t); \quad y_0 = b, \quad t > 0, \quad (1)$$

where ρ_c and $\sigma > 0$ are unknown fixed parameters, and $\{W(t) : t \geq 0\}$ is a standard Brownian motion. The unique solution for $\{y(t) : t \geq 0\}$ in the mean square sense (Arnold, 1974) is given by

$$y_t = e^{\rho_c t} b + \sigma \int_0^t e^{\rho_c(t-s)} dW(s) = e^{\rho_c t} b + \sigma J_{\rho_c}(t), \quad (2)$$

where $J_{\rho_c}(t) = \int_0^t e^{\rho_c(t-s)} dW(s)$. Note that $J_{\rho_c}(t) \sim N(0, (e^{\rho_c t} - 1)/2\rho_c)$.

Suppose one is interested in estimating ρ_c based on a single observed path $\{y(t)\}_{0 \leq t \leq T}$. The mean squared estimator of ρ is given by

$$\hat{\rho}_c = \int_0^T y(t) dy(t) / \int_0^T y(t) dt. \quad (3)$$

which is also the unrestricted maximum likelihood estimator if $b = 0$.

The discrete representation of such process is given by

$$y_{t,h} = e^{\rho_c h} y_{(t-1),h} + u_{t,h}, \quad t > 0, \quad y_0 = b, \quad (4)$$

where $u_{t,h} \sim N(0, \sigma^2(e^{2\rho_c h} - 1)/2\rho_c)$ and h is the sampling interval.

In this discretized version of the problem, one aims to estimate $\rho_h = e^{\rho_c h}$ given the observations $\{y_{t,h}\}_{t=0}^n$, where $n = T/h$. The minimum squared error estimator, which is also the conditional (on y_0) maximum likelihood solution, is given by

$$\hat{\rho}_h = \sum_{t=1}^n y_{t,h} y_{(t-1),h} / \sum_{t=1}^n y_{(t-1),h}^2.$$

*corresponding author: pinheiro@ime.unicamp.br

Perron (1991) studies the limit distribution of $n(\hat{\rho}_h - \rho_h)$ under (4), when $h \rightarrow 0$ and fixed T , and proves that it is identical to the limiting distribution of $T(\hat{\rho}_c - \rho_c)$ under (1). Suppose one is interested in estimating and testing functions f in the model defined by:

$$dy_i(t) = f_i(t)dt + \varepsilon_i(t)dt, \quad t \in [0, 1], \quad i = 1, \dots, r, \quad (5)$$

where r is the number of curves being compared and $\{\varepsilon(t) : t \geq 0\}$ is a CAR(1) model. The aforementioned CAR(1) is also called the Ornstein-Uhlenbeck process and is the only stationary solution of the PDE

$$d\varepsilon(t) + \alpha\varepsilon(t)dt = \sigma dW(t), \quad (6)$$

where α and σ are unknown positive parameters. Note that

$$\mathbb{E}[\varepsilon(t)|\varepsilon(0)] = e^{-\alpha t}\varepsilon(0) \quad (7)$$

$$\text{Var}[\varepsilon(t)|\varepsilon(0)] = \frac{\sigma^2}{2\alpha}(1 - e^{-2\alpha t}). \quad (8)$$

Moreover, $\{\varepsilon(t)\}$ can be written as

$$\varepsilon(t) = e^{-\alpha t}\varepsilon(0) + \sigma \int_0^t e^{-\alpha(t-s)} dW(s) = e^{-\alpha t}\varepsilon(0) + \sigma J_\alpha(t)$$

where $J_\alpha(t) = \int_0^t e^{-\alpha(t-s)} dW(s)$, which is distributed as $N(0, (1 - e^{-2\alpha t})/2\alpha)$. This solution is stationary, so that $\alpha > 0$ and $\varepsilon(t) \sim N(0, \sigma^2/2\alpha) \quad \forall t \geq 0$. Consequently,

$$\begin{aligned} \mathbb{E}[y_i(t)|f_i(t), \sigma^2, \alpha] &= f_i(t), \\ \text{Var}[y_i(t)|f_i(t), \sigma^2, \alpha] &= \sigma^2/(2\alpha) \text{ and} \\ \text{Corr}[y_i(s), y_i(t)|f_i(t), \sigma^2, \alpha] &= e^{-\alpha(t-s)}, \text{ for } s < t. \end{aligned}$$

2 Estimation and Testing

Suppose the model defined by (5). If the sample on the CAR(1) is equally spaced, i.e. such that $h = 1/n$ one can write $\rho = \rho(\alpha, h) = e^{-\alpha h}$. Given the discrete process variance σ_p^2 , one can write $\sigma_p^2 = \sigma^2/(2\alpha)$, and $\sigma_p^2(1 - e^{-2\alpha h}) = \sigma_p^2(1 - \rho^2)$.

Following (4), we discretize the model as

$$y_{i,t} = f_{i,t} + \varepsilon_{i,t}, \quad i = 1, \dots, r, \quad (9)$$

where $\varepsilon_{i,t} = \rho\varepsilon_{i,t-1} + u_{i,t}$ are independent CAR(1) processes, $i = 1, \dots, r$, and the $u_{i,t} \sim (0, \sigma_u^2)$ uncorrelated with $\varepsilon_{i,s}$, $s < t$ for each i . The Fisher information matrix for this model is given by:

$$I(f_t, \rho, \sigma_u^2) = \begin{bmatrix} \frac{1}{\sigma_u^2} (1 - \rho^2 + (n-1)(1-\rho)^2) & 0 & 0 \\ 0 & \frac{n-1 + (3-n)\rho^2}{(1-\rho^2)^2} & \frac{1}{\sigma_u^2(1-\rho^2)} \\ 0 & \frac{1}{\sigma_u^2(1-\rho^2)} & \frac{n}{2\sigma_u^4} \end{bmatrix},$$

which, being block-diagonal, justifies applying diverse methods for f_t and (ρ, σ_u^2) . For instance, we estimate the former by wavelets, and the latter by ML.

The procedure can be resumed as follows:

- (E1) Initial solution for $\rho : \hat{\rho} \in (-1, 1)$;
- (E2) Compute $y_t - \hat{\rho}y_{t-1} = f_t - \hat{\rho}f_{t-1} + u_t$, i.e., $z_t = g_t + u_t$, and estimate g (g_t) by \hat{g} (\hat{g}_t);
- (E3) Estimate f by $\hat{f}_t = \hat{g}_t + \hat{\rho}\hat{f}_{t-1}$, with $\hat{f}_0 = y_0$;
- (E4) Estimate ρ by $\hat{\rho} = \sum_{t=2}^n e_t e_{t-1} / \sum_{t=2}^n e_t^2$, where $e_t = y_t - \hat{f}_t$;
- (E5) Testing convergence by subsequent estimated values of ρ ;

(E6) Repete steps (2)-(5) until convergence is attained, or the maximum number of iterations is reached.

Remarks:

1. In step (2) one may estimate g linearly on nonlinearly.
2. The variance σ_u^2 must be estimated in each iteration if non-linear wavelet estimators are used in (2). Otherwise, one only needs it at the end of the process. In the simulation studies and in the application, we compared MAD and STD estimates for σ_u^2 (Vidakovic, 1999 pp. 196-7).

It is known that high-dimensional models, and functional models as well, pose a problem for the classical criteria such as Neyman optimality. For that reason some shrinkage must be applied in order to get statistically sound solutions. In the HANOVA setup, Fan (1996) and Fan and Lin (1998) present adaptive Neyman tests for high-dimensional parameters and curves, respectively.

Abramovich et al. (2004) proposes a FANOVA model for

$$dy_i(t) = f_i(t)dt + \varepsilon_i(t)dt, \quad t \in [0, 1], \quad i = 1, \dots, r, \quad (10)$$

where r is the number of curves being compared and $\{\varepsilon(t) : t \geq 0\}$ is a Brownian motion. (10) and (5) may be seen as equivalent models except for the error structure.

The FANOVA decomposition is given by

$$f_i(t) = m_0 + \mu(t) + a_i + \gamma_i(t), \quad i = 1, \dots, r; \quad t \in [0, 1] \quad (11)$$

where: m_0 is the overall mean; $\mu(t)$ is the main effect in t ; a_i is the main effect in i ; $\gamma_i(t)$ is the interaction between i e t , with the following identifiability conditions

$$\int_0^1 \mu(t)dt = 0; \quad \sum_{i=1}^r a_i = 0; \quad \sum_{i=1}^r \gamma_i(t) = 0; \quad \int_0^1 \gamma_i(t)dt = 0, \quad \forall i = 1, \dots, r; \quad t \in [0, 1]. \quad (12)$$

One would be interested in hypotheses such as:

$$H_0 : \mu(t) \equiv 0, \quad t \in [0, 1]; \quad (13)$$

$$H_0 : a_i = 0, \quad i = 1, \dots, r; \quad \text{and} \quad (14)$$

$$H_0 : \gamma_i(t) \equiv 0, \quad i = 1, \dots, r \quad t \in [0, 1]. \quad (15)$$

While (14) can be treated as the usual parametric hypotheses, (13) (15) are intrinsically functional. Donoho and Johnstone (1995, 1998) and Spokoiny (1996) present optimal minimax rates in Besov spaces which are attained by wavelet procedures. For a significance level $\alpha \in (0, 1)$ let ϕ^* be the test defined by

$$\phi^* = \begin{cases} \mathbf{1} \{T(j(s)) > v_0(j(s))z_{1-\alpha}\} & \text{if } p \geq 2; \text{ or} \\ \mathbf{1} \{T(j(s)) + Q(j(s)) > \sqrt{v_0^2(j(s)) + w_0^2(j(s))}z_{1-\alpha}\} & \text{if } 1 \leq p < 2, \end{cases} \quad (16)$$

where p , q , s and C are considered known. We refer the readers to Abramovich et al. (2004) for details. This test is proven to be optimal in the minimax sense. The non-adaptative test also proposed by Abramovich et al. (2004), which is optimal as well, is given by $\phi_\eta^* = 1$ if:

$$\phi_\eta^* = \max_{j_{\min} \leq j(s) \leq j_\eta - 1} \left\{ \frac{T(j(s)) + Q(j(s))}{\sqrt{v_0^2(j(s)) + w_0^2(j(s))}} \right\} > \sqrt{2 \ln \ln \eta^{-2}}.$$

If one knows that $p \geq 2$, then $\phi_\eta^* = 1$ if

$$\phi_\eta^* = \max_{j_{\min} \leq j(s) \leq j_\eta - 1} \left\{ \frac{T(j(s))}{\sqrt{v_0^2(j(s))}} \right\} > \sqrt{2 \ln \ln \eta^{-2}}.$$

One assumes above that the $f_i(t)$ belong to a Besov ball of radius $C > 0$, in $[0, 1]$, $B_s^{p,q}(C)$, where $s > 1/p$ and $1 \leq p, q \leq \infty$.

For the dependent error model (5), a two-step iterative procedure is employed, where in each iteration ρ and f are successively estimated by a Cochrane-Orkutt type procedure, specified in (E1)-(E6), employing the estimation (and testing) procedures proposed by Abramovich et al. (2004) for f .

One can then prove that reasonable error norms are minimized by this procedure. In particular, it can be proven that the L^2 error norm is improved in each iteration.

3 Simulation Studies

We present simulation studies to evaluate the testing procedure. Twelve classical test functions (Figure 1), five sample sizes ($n = 512; 1024; 2048; 4096; 8192$), three signal-to-noise ratios (SNR = 1; 3; 7), two values of ρ (0.99 and 0.9999) and three wavelets bases ('db3'; 'db6'; and 'sym8') are considered. For each combination, 1000 replications were taken.

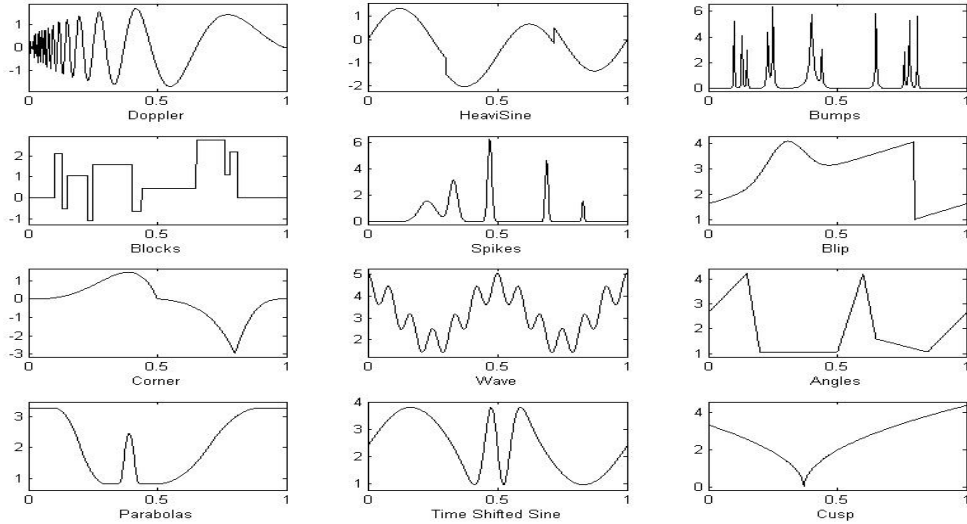


Figure 1: Test functions

Since $\alpha = -n \log \rho$ one has for $\rho = 0.99$ and $n = 512; 1024; 2048; 4096; 8192$, $\alpha = 5.14; 10.29; 20.58; 41.16; 82.33$, respectively. For $\rho = 0.9999$, one has $\alpha = 0.051; 0.102; 0.204; 0.409; 0.819$, respectively.

Moreover, both linear (Antoniadis et al., 1994) and non-linear (Spokoyny, 1996; Abramovich et al., 2004) steps are implemented. For the former projection is made in V_5 for $n = 512$, V_6 for $n = 1024; 2048$ and V_7 for $n = 4096; 8192$ are employed. For the latter, thresholding in the levels 4–7 for $n = 512; 1024; 2048$ and 5–8 for $n = 4096; 8192$ are performed. In the last iteration, after ρ is estimated, the function is estimated by thresholding either term-by-term (Spokoyny, 1996; Abramovich et al., 2004) or by blocks (Cai, 1999, 2002).

Data was generated by the model

$$y_t = f_t + \varepsilon_t, \quad t = 1, \dots, n, \quad (17)$$

where $\varepsilon_t = \rho \varepsilon_{t-1} + u_t$ is a discretized CAR(1), $\rho = e^{-\alpha/n}$, $u_t \sim N(0, (1 - \rho^2)\sigma^2/2\alpha)$, $\varepsilon_0 \sim N(0, \sigma^2/2\alpha)$ and f_t a test function.

For each combination of ρ and n , one uses $\sigma^2 = 1$ and rescales the test function to get the desired SNR. In each estimation procedure, 50 randomly selected values in $(-1, 1)$ are used as initial values of $\hat{\rho}$. MAD estimates of σ_u are employed for the non-linear estimates. The stopping criterium was a difference on the subsequent ρ estimates smaller than $< 10^{-15}$ or 250 iterations.

A smaller preliminary simulation was performed with the single aim of assessing the real need of estimating ρ . Table 1 shows the performance of the estimators of f as a function of the employed value of ρ . 1000 replications on each combination of $f(t) = \sin(2\pi t)$, $n = 1025$, SNR = 7 and $\rho = 0.99; 0.999; 0.9999$ are taken. The 'db6' basis is used in a term-by-term non-linear procedure on levels 5 to 7 (Abramovich et al., 2004) for the final f estimation. The iterations were made with thresholding from levels 4 to 7. Moreover, to show the effects of ignoring the dependence on ε , twelve estimators are compared. Eleven fixed values for ρ are considered: $-0.9, -0.7, -0.5, -0.3, -0.1, 0, 0.1, 0.3, 0.5, 0.7, 0.9$. The Integrated Mean Squared Error (IMSE) is used to compare the results. We summarize the results in Table 1 through the IMSE ranks for each case ($\rho = 0.99; 0.999; 0.9999$ or, analogously, $\alpha = 10.2915; 1.0245; 0.1024$). One notices that the proposed method has in general a better performance when compared to the ad-hoc procedure based on a fixed value of ρ .

Table 1: Average and Median Rank on the proposed IMSE (out of 1000 replications) $f(t) = \sin(2\pi t)$, SNR = 7, 'db6' and $n = 1025$.

Rank \ ρ	0.99	0.999	0.9999
Average	11.3820	11.1420	11.1370
Median	11	12	12

We present in Table 2 an overview for all test functions. The lines within each column represent the number of times (out of 15) in which the titled technique or basis achieved the best performance. The Appendix has a detailed presentation for the *Doppler* test function. The details for the other test functions can be made available as Supplementary Material.

Some of the simulation results were expected. For instance, for either value of ρ , the bias of the linear estimator of ρ generally decreases in the SNR and in the sample size. Some order discrepancies on n are observed, but the fact that the functional projection is made in a fixed V_j can be taken as cause for them. A similar behavior is seen when the non-linear estimator is employed, albeit in much milder terms. However, one should pay special attention to the thresholding procedure. When comparing the linear and non-linear procedures, the latter is the best performer. For $\rho = 0.99$, it attains precisions of two or more decimal places against one for the former whenever $n \geq 1024$. Analogous results are seen for $\rho = 0.9999$. In some specific situations the linear estimator has a better performance but, since this can not be predicted in practice, the non-linear should be employed. Another conclusion regarding the estimation of ρ is that it is heavily influenced by any bias on the estimation of f , be it by *mistaken* projection or over- and under-shrinkage. No significant effect of the initial value of ρ has been found.

The results regarding linear vs non-linear functional estimation are somewhat similar to the ones for ρ . There are cases in which the linear estimator outperforms the non-linear estimator. However, there are no instance of really poor performance by the non-linear estimator while the linear estimator fails severely for some test functions. Moreover, in the case where the linear estimators have a better performance, the differences are small. The numerical differences due to the bases are small but favor in general the 'db6' and 'db3' bases.

The overall recommendation is to use the term-by-term thresholding wavelet estimator for all but the last iteration. Then after the final estimation of ρ , a blocking-thresholded estimator of f yields the best performance.

4 Application to SONDA's Environmental Data

The data was obtained from SONDA (National System of Environmental Data, INPE-Brazil, <http://sonda.ccst.inpe.br>). The SONDA network has minute-by-minute environmental data. We analyze the variables air temperature at surface, air relative humidity, and air pressure. The four initial months for each season, March, June, September and December, were selected.

The Weather stations in Brasília, Ourinhos and São Luiz were chosen, given their latitude, longitude and altitude characteristics. The integrity and the nature and consistency of the data were also important factors in the choice of cities and variables analyzed. We consider 22.75 days

Table 2: Overview of the Simulation Studies for Estimation of f, ρ .

Type(1)	Bias and MSE		Smallest Bias		Smallest MSE		IMSE		Smallest IMSE			
	MSE	NL	'db3'	'db6'	'sym8'	'db3'	'db6'	'sym8'	NL blocks	'db3'	'db6'	'sym8'
Do1	11	2	9	4	2	11	2	8	2	5	8	8
Do2	10	9	6	0	1	5	9	15	1	5	9	9
He1	15	4	8	3	9	5	1	4	0	11	4	4
He2	10	5	9	1	1	5	9	12	9	5	1	1
Bu1	9	5	7	3	10	2	3	12	10	2	3	3
Bu2	13	7	8	0	1	5	9	15	14	1	0	0
Bk1	11	7	7	1	6	7	2	9	4	4	7	7
Bk2	14	11	3	1	11	3	1	15	12	0	3	3
Sp1	11	6	6	3	6	7	2	7	1	6	8	8
Sp2	6	2	8	5	2	8	5	12	5	3	7	7
Bp1	13	7	7	1	4	8	3	8	2	8	5	5
Bp2	7	10	5	0	10	5	0	13	7	4	4	4
Co1	15	6	3	6	3	7	5	4	13	0	2	2
Co2	14	8	4	3	7	5	3	6	2	9	4	4
Wa1	15	2	11	2	2	12	2	5	3	12	0	0
Wa2	11	2	5	8	4	5	6	12	3	12	0	0
An1	15	9	5	1	6	8	1	2	0	11	4	4
An2	12	8	4	3	6	4	5	10	4	8	3	3
Pa1	15	6	6	3	3	11	1	11	0	14	1	1
Pa2	14	4	3	8	4	4	7	9	2	11	2	2
Ts1	15	5	6	4	4	8	3	3	0	13	2	2
Ts2	12	4	6	5	2	8	5	10	4	8	5	5
Cu1	15	5	6	4	4	8	3	5	0	11	4	4
Cu2	12	3	12	0	2	13	0	7	6	4	5	5

(1) Do* - Doppler; He* - Heavisine; Bu* - Bumps; Bk* - Blocks; Sp* - Spikes; Bp* - Blip; Co* - Corner; Wa* - Wave; An* - Angles; Pa* - Parabolae; Ts* - Time Shifted Sine; Cu* - Cusp.

For all cases, if * = 1, $\rho = 0.99$. If * = 2, $\rho = 0.9999$. NL means (nonlinear) thresholding.

Table 3: Latitude, longitude and altitude characteristics and Estimates of ρ based on ‘db6’. $\hat{\rho}_3$, $\hat{\rho}_6$, $\hat{\rho}_9$ e $\hat{\rho}_{12}$ are the ρ estimates for March, June, September and December, respectively. The analysis is based upon $n = 2^{15}$ data points, which corresponds to 22.75 days for each month. The iterative procedure employs term-by-term thresholding from levels 5 to 8.

Station	Lat.(S)	Long.(W)	Alt.(m)	Estimator	Temperature	Humidity	Pressure
Brasília	15°36’	47°42’	1023	$\hat{\rho}_3$	0.9996	0.8807	0.9992
				$\hat{\rho}_6$	0.9996	0.9764	0.9992
				$\hat{\rho}_9$	0.9995	0.9968	0.9994
				$\hat{\rho}_{12}$	0.9994	0.9499	0.9993
Ourinhos	22°56’	49°53’	446	$\hat{\rho}_3$	0.9988	0.9975	0.9985
				$\hat{\rho}_6$	0.9992	0.9978	0.9983
				$\hat{\rho}_9$	0.9990	0.9963	0.9985
				$\hat{\rho}_{12}$	0.9989	0.9932	0.9987
São Luiz	02°35’	44°12’	40	$\hat{\rho}_3$	0.9982	0.9913	0.9995
				$\hat{\rho}_6$	0.9988	0.9932	0.9985
				$\hat{\rho}_9$	0.9005	0.9960	0.9989
				$\hat{\rho}_{12}$	0.9981	0.9972	0.9981

for each month, which provides a total of $2^{15} = 32,768$, starting in the first hour of the first day of each selected month of 2009.

The term-to-term thresholding wavelet estimator was employed based on the ‘db6’ basis. Five initial values for ρ are employed, randomly generated from a $U(-1, 1)$. Thresholding is performed on the levels 5 to 8 until ρ is estimated. After that, in the last iteration, only levels 8 and 9 were thresholded, as proposed by Abramovich et al. (2004).

Table 3 presents the estimates for ρ for the SONDA’s stations. First, we’d like to emphasize that the final estimate does not depend on its initial value, i.e., in all cases the five initial values yield the same ρ estimates. The general conclusion is that a reasonable variation is observed in the estimated values of ρ which corroborates the necessity of adjusting the data set to their effects. Moreover, high values of ρ are observed.

Some specific results should be discussed. The three cities, which have very different weather conditions, do present different behaviors in the ρ values as well. For instance, Brasília presents very stable values of ρ for temperature and pressure, but humidity’s ρ vary during the year. Ourinhos has similar behavior for the values of ρ over time and among the environmental variables. São Luiz presents reasonably stable values of ρ for humidity and pressure, but temperature in September has quite a different value of ρ from the rest of the year.

In the remaining text we analyze the data of Brasília. Figures 2, 3 and 4 show the temperature, humidity and atmospheric pressure observed and estimated the first 22 days of the month of March 2009 for the city of Brasília, respectively. A noisy curve of interpolated observed values and a smoothed estimated curve is presented for each day. Figures 5, 6 and 7 present the estimates for the Brasília’s daily curves of temperature, humidity and pressure, respectively. One sees some similar behavior on the daily temperature and atmospheric pressure curves for each variable within each month, with some exceptions. In general, these daily curves are very regular with one local minimum and maximum per day for the temperature and two local maxima and minima for the pressure. The humidity curves present much wider daily amplitude and much less regular behavior within each month, specially for the rainy season months, i.e. March and December.

Average Brasília daily estimates curves for the first 22 days of March, June, September and December 2009 are shown in Figure 8. One sees that June presents the coldest days, and September, the hottest days. The month of September is usually the driest, and December the wettest. Finally the months of March and December present lower atmospheric pressures compared to June and September.

To verify that the curves of climatic variables have identical behavior from one year to another applied the test described in the proposed model to the observed data in 2009 and 2010 in Brasília. Has taken the observed curves for June and September 2010 from Brasília to perform this test.

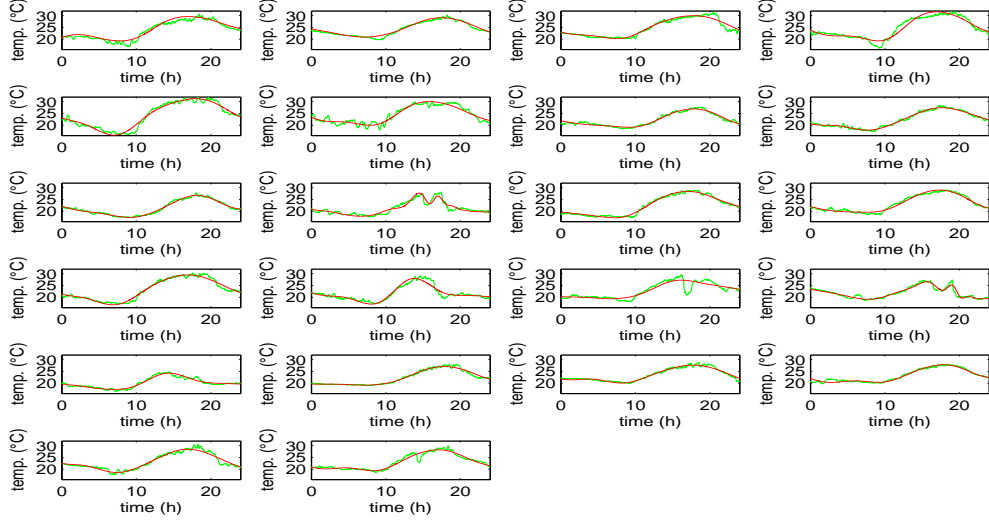


Figure 2: Brasília's estimated and observed temperature curves for the month of March 2009.

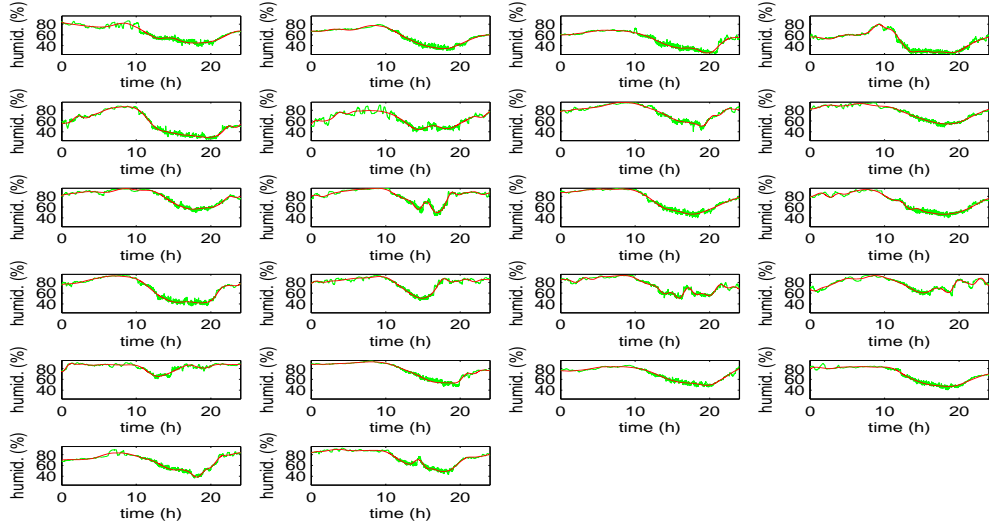


Figure 3: Brasília's estimated and observed humidity curves for the month of March 2009.

The data for March are incomplete and of December were lost. Since the data are correlated, one can not perform the test developed in (Abramovich et al., 2004) directly. Therefore, before performing the test made the transformation $y_t - \hat{\rho}y_{t-1}$, $t = 1, 2, \dots, n$ in the observed data for the uncorrelated errors. Thus, $y_t - \hat{\rho}y_{t-1} = f_t - \hat{\rho}f_{t-1} + u_t \iff z_t = g_t + u_t$, in which errors u_t have approximately distribution $N(0, \sigma_u^2)$. To perform the test replaces the function f by the curve estimated for 2009. Thus we tested

$$H_0 : z - g \equiv \text{Constant} \quad \text{versus} \quad H_1 : (z - g - \text{Constant}) \in \mathcal{F}(\varrho),$$

with significance $\alpha = 5\%$. The test result for June and September to the station of Brasília are in Table 4.

In all cases, the null hypothesis was rejected. Thus the curves observed in the months of June

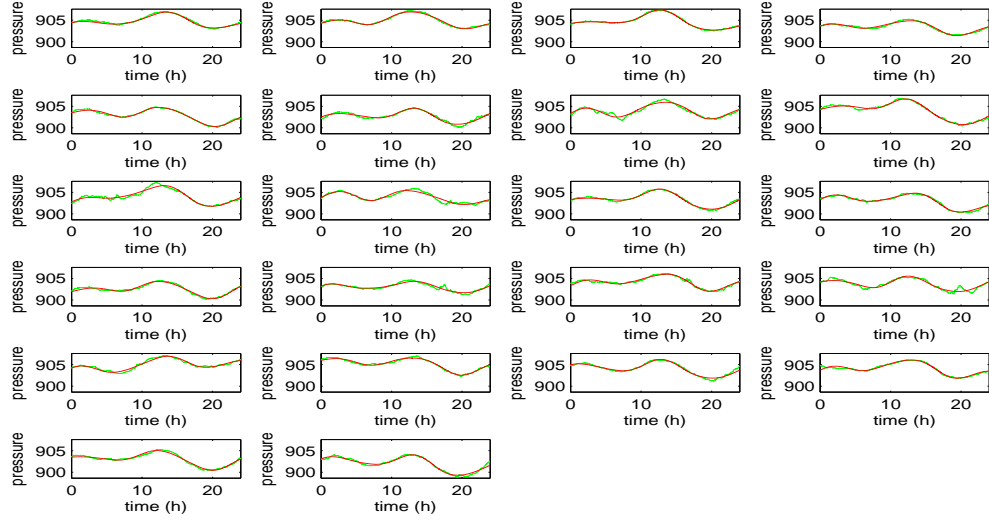


Figure 4: Brasília's estimated and observed air pressure curves for the month of March 2009.

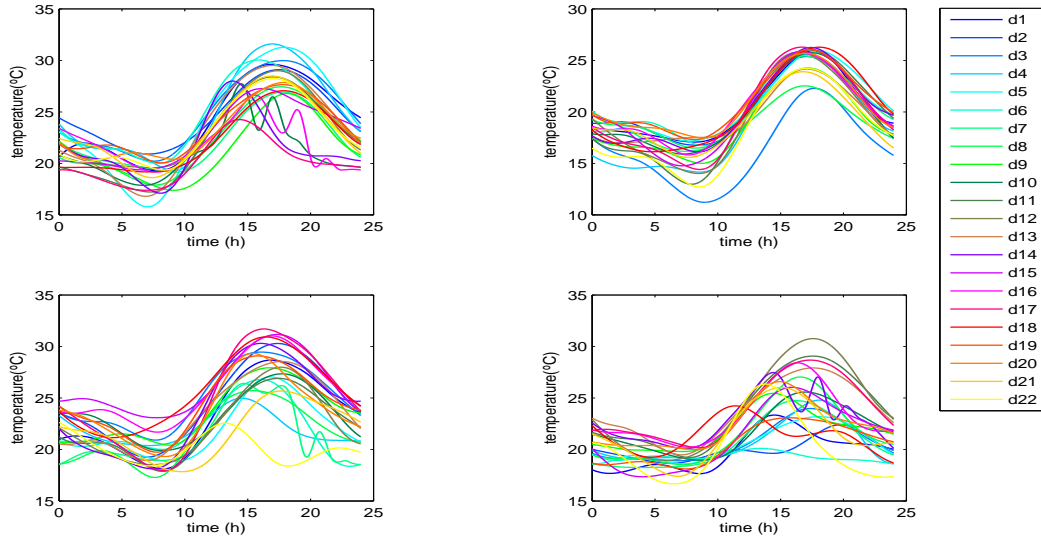


Figure 5: Brasília's Daily Estimated temperature curves for March, June, September and December of 2009. d_i represents days i .

and September 2010 are different curves observed in the same period of 2009.

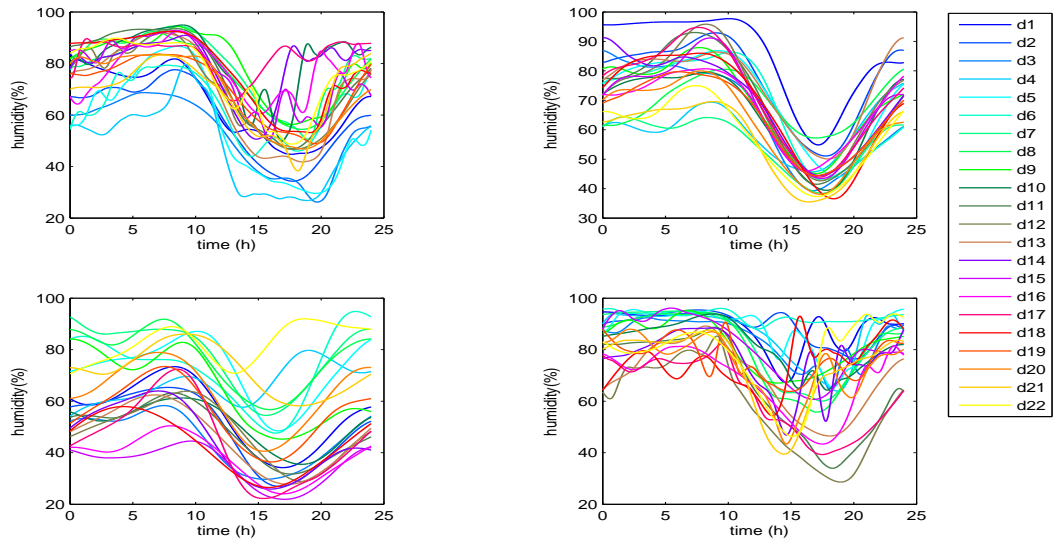


Figure 6: Brasília's Daily Estimated humidity curves for March, June, September and December of 2009. d_i represents days i .

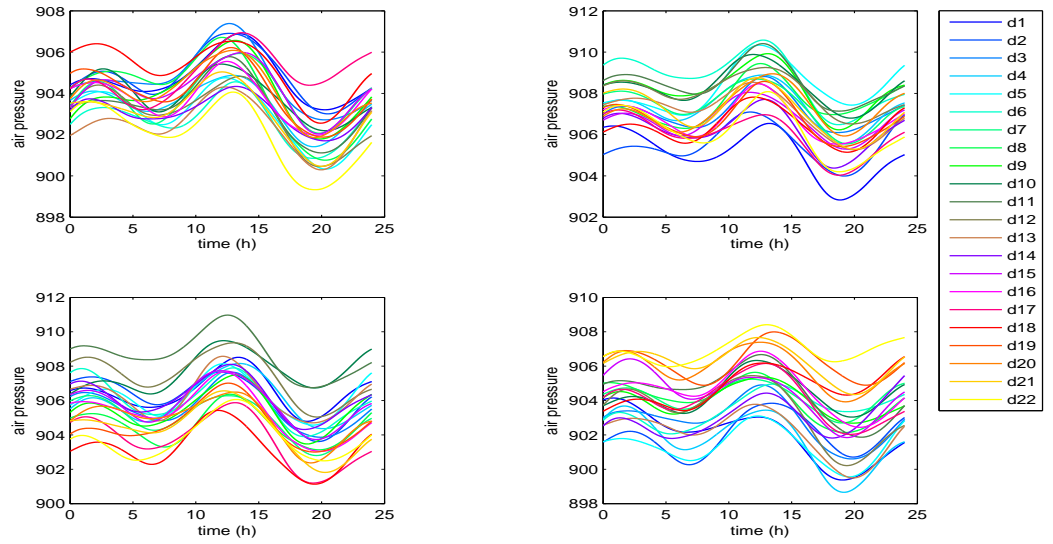


Figure 7: Brasília's Daily Estimated atmospheric pressure curves for March, June, September and December of 2009. d_i represents days i .

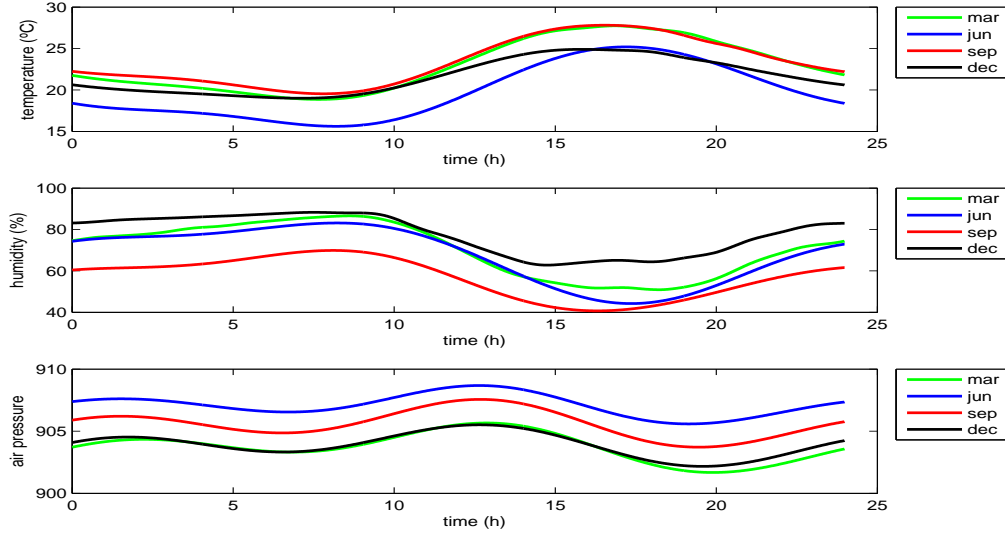


Figure 8: Brasília's Mean Estimated curves for the first 22 days of March, June, September and December of 2009. Separate Plots for mean temperature, humidity and pressure curves are presented.

Table 4: Test results $H_0 : z - g \equiv \text{Constant}$ versus $H_1 : (z - g - \text{Constant}) \in \mathcal{F}(\varrho)$ with significance $\alpha = 5\%$. $T(j(6)) + Q(j(6))$ is the value of statistics and $\sqrt{v_0^2(6) + w_0^2(6)}z_{0.95}$ is the critical value

		Temperature	Humidity	Pressure
June	$T(j(6)) + Q(j(6))$	213.43	81,900,00	215.69
	$\sqrt{v_0^2(6) + w_0^2(6)}z_{0.95}$	0.22	2.99	0.08
September	$T(j(6)) + Q(j(6))$	466.01	3,396.40	43.94
	$\sqrt{v_0^2(6) + w_0^2(6)}z_{0.95}$	0.20	1.97	0.07

5 Discussion

The analysis of functional data has become more common in the last decades due to the exponential increase in computing power, which has driven the also increasing large datasets' acquisition and the development of appropriate statistical analysis tools. We present a modification of optimal wavelet procedures (Abramovich et al., 2004) to deal with dependent errors. The theoretical advantages of correctly estimating the error dependence are shown, by simulation and application to real data set, to be also quite relevant in practice.

References

- Abramovich, F., Antoniadis, A., Sapatinas, T., and Vidakovic, B. (2004). Optimal testing in a fixed-effects functional analysis of variance model. *Int. J. Wavelets Multiresolut. Inf. Process.*, 2(4):323–349.
- Antoniadis, A., Grégoire, G., and McKeague, I. W. (1994). Wavelet methods for curve estimation. *J. Amer. Statist. Assoc.*, 89(428):1340–1353.
- Arnold, L. (1974). *Stochastic differential equations: theory and applications*. Wiley-Interscience [John Wiley & Sons], New York. Translated from the German.
- Cai, T. T. (1999). Adaptive wavelet estimation: a block thresholding and oracle inequality approach. *Ann. Statist.*, 27(3):898–924.
- Cai, T. T. (2002). On block thresholding in wavelet regression: adaptivity, block size, and threshold level. *Statist. Sinica*, 12(4):1241–1273.
- Donoho, D. L. and Johnstone, I. M. (1995). Adapting to unknown smoothness via wavelet shrinkage. *J. Amer. Statist. Assoc.*, 90(432):1200–1224.
- Donoho, D. L. and Johnstone, I. M. (1998). Minimax estimation via wavelet shrinkage. *Ann. Statist.*, 26(3):879–921.
- Fan, J. (1996). Test of significance based on wavelet thresholding and Neyman's truncation. *J. Amer. Statist. Assoc.*, 91(434):674–688.
- Fan, J. and Lin, S.-K. (1998). Test of significance when data are curves. *J. Amer. Statist. Assoc.*, 93(443):1007–1021.
- Perron, P. (1991). A continuous time approximation to the unstable first-order autoregressive process: the case without an intercept. *Econometrica*, 59(1):211–236.
- Spokoiny, V. G. (1996). Adaptive hypothesis testing using wavelets. *Ann. Statist.*, 24(6):2477–2498.

Appendix

We show below some figures and tables for the Doppler function simulation results. Results for the other functions were qualitatively equivalent, and are available as supplementary material.

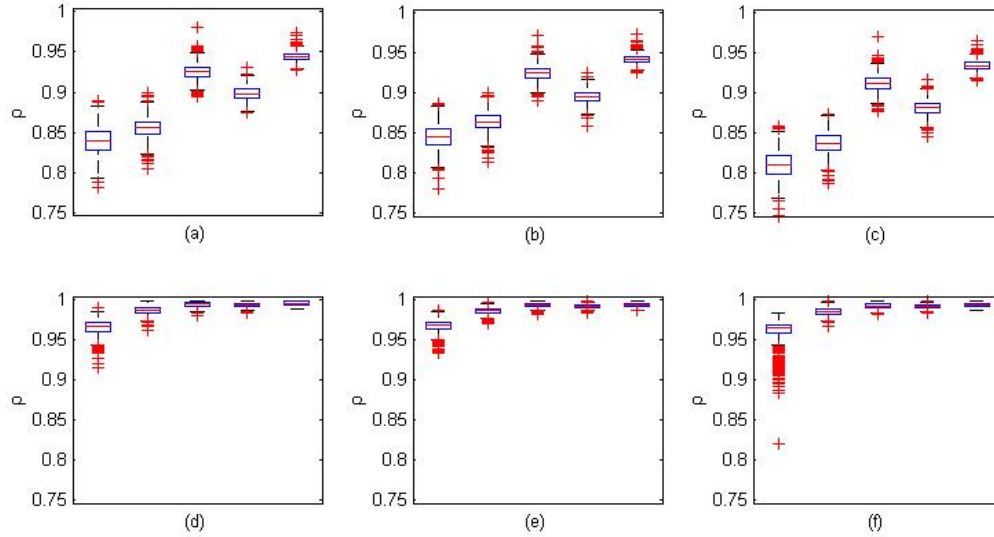


Figure 9: Box-Plots for $\hat{\rho}$. Doppler function, $\rho = 0.99$, $\text{SNR} = 1$. 1000 replications. 50 initial values randomly chosen from $U(-1, 1)$. Panels: (a) Linear functional step and 'db3'; (b) Linear functional step and 'db6'; (c) Linear functional step and 'sym8'; (d) Nonlinear functional step and 'db3'; (e) Nonlinear functional step and 'db6'; (f) Nonlinear functional step and 'sym8'. In each panel box-plots for sample sizes $n = 512; 1024; 2048; 4096; 8192$ are shown from left to right.

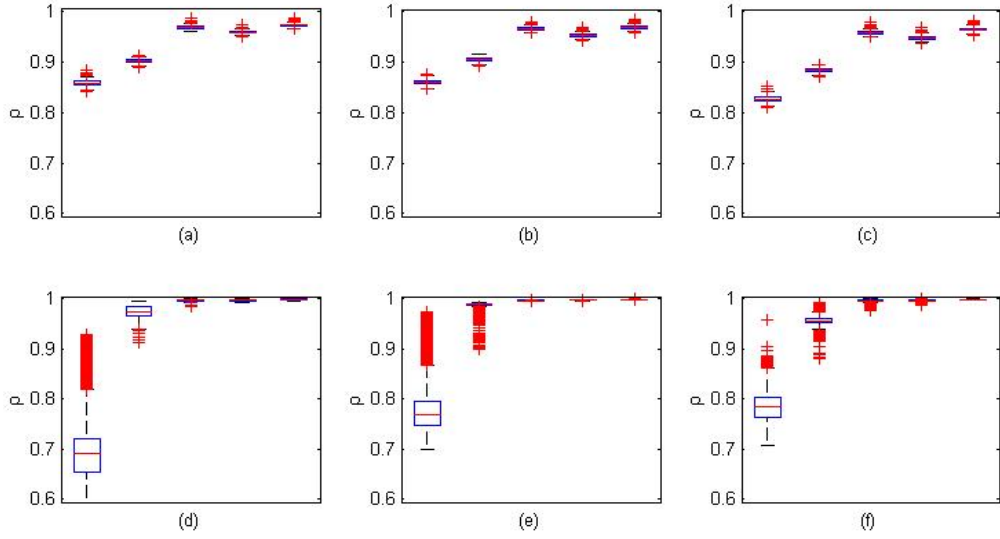


Figure 10: Box-Plots for $\hat{\rho}$. Doppler function, $\rho = 0.99$, SNR = 3. 1000 replications. 50 initial values randomly chosen from $U(-1, 1)$. Panels: (a) Linear functional step and 'db3'; (b) Linear functional step and 'db6'; (c) Linear functional step and 'sym8'; (d) Nonlinear functional step and 'db3'; (e) Nonlinear functional step and 'db6'; (f) Nonlinear functional step and 'sym8'. In each panel box-plots for sample sizes $n = 512; 1024; 2048; 4096; 8192$ are shown from left to right.

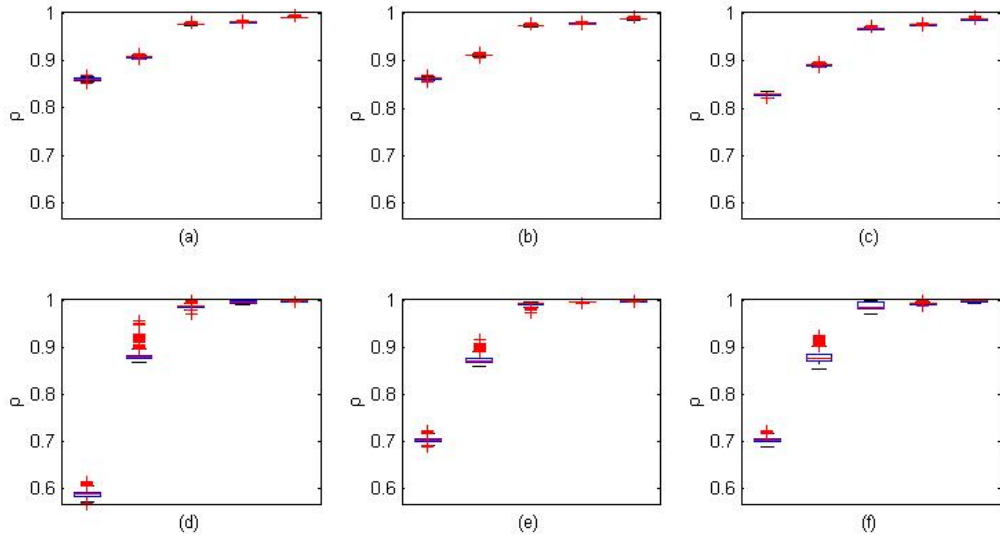


Figure 11: Box-Plots for $\hat{\rho}$. Doppler function, $\rho = 0.99$, SNR = 7. 1000 replications. 50 initial values randomly chosen from $U(-1, 1)$. Panels: (a) Linear functional step and 'db3'; (b) Linear functional step and 'db6'; (c) Linear functional step and 'sym8'; (d) Nonlinear functional step and 'db3'; (e) Nonlinear functional step and 'db6'; (f) Nonlinear functional step and 'sym8'. In each panel box-plots for sample sizes $n = 512; 1024; 2048; 4096; 8192$ are shown from left to right.

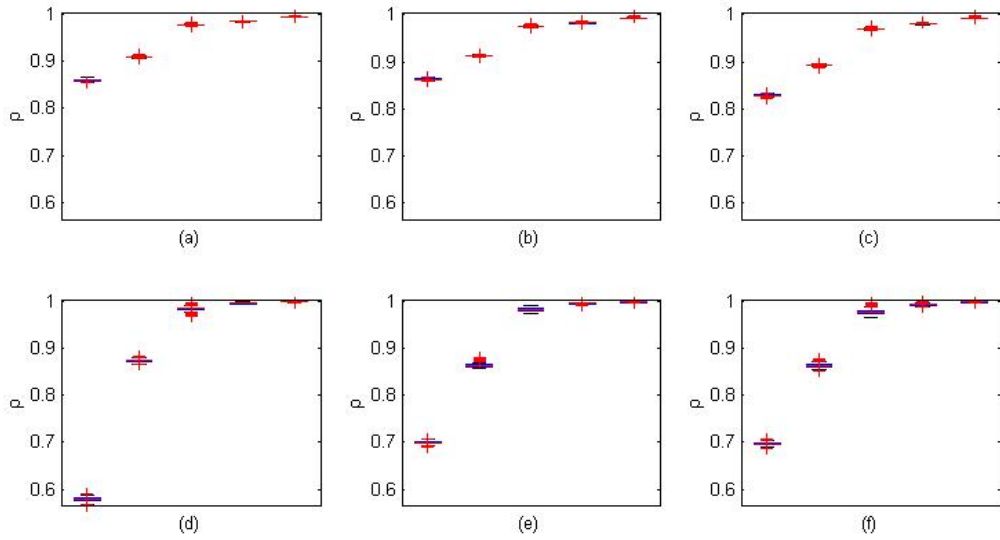


Figure 12: Box-Plots for $\hat{\rho}$. Doppler function, $\rho = 0.9999$, SNR = 1. 1000 replications. 50 initial values randomly chosen from $U(-1, 1)$. Panels: (a) Linear functional step and 'db3'; (b) Linear functional step and 'db6'; (c) Linear functional step and 'sym8'; (d) Nonlinear functional step and 'db3'; (e) Nonlinear functional step and 'db6'; (f) Nonlinear functional step and 'sym8'. In each panel box-plots for sample sizes $n = 512; 1024; 2048; 4096; 8192$ are shown from left to right.

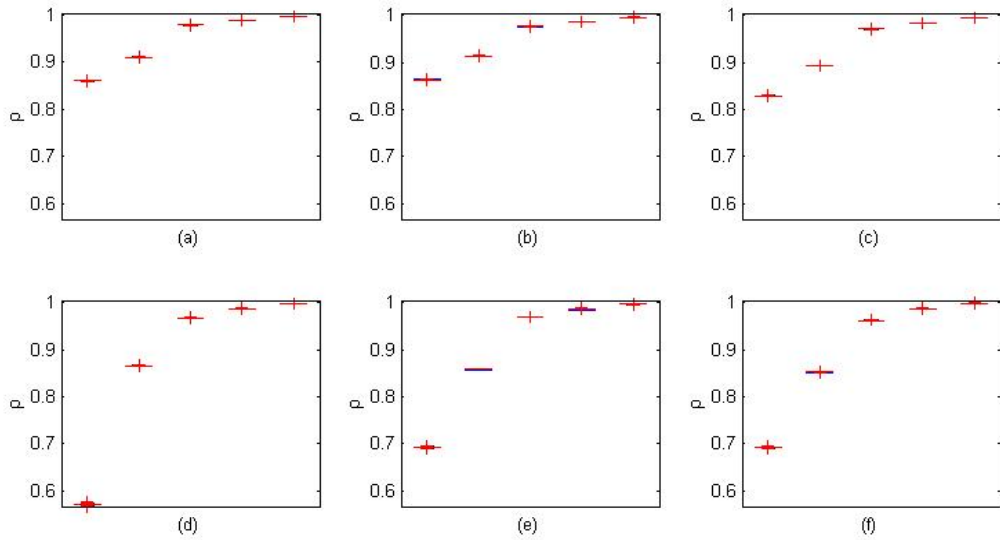


Figure 13: Box-Plots for $\hat{\rho}$. Doppler function, $\rho = 0.9999$, SNR = 3. 1000 replications. 50 initial values randomly chosen from $U(-1, 1)$. Panels: (a) Linear functional step and 'db3'; (b) Linear functional step and 'db6'; (c) Linear functional step and 'sym8'; (d) Nonlinear functional step and 'db3'; (e) Nonlinear functional step and 'db6'; (f) Nonlinear functional step and 'sym8'. In each panel box-plots for sample sizes $n = 512; 1024; 2048; 4096; 8192$ are shown from left to right.

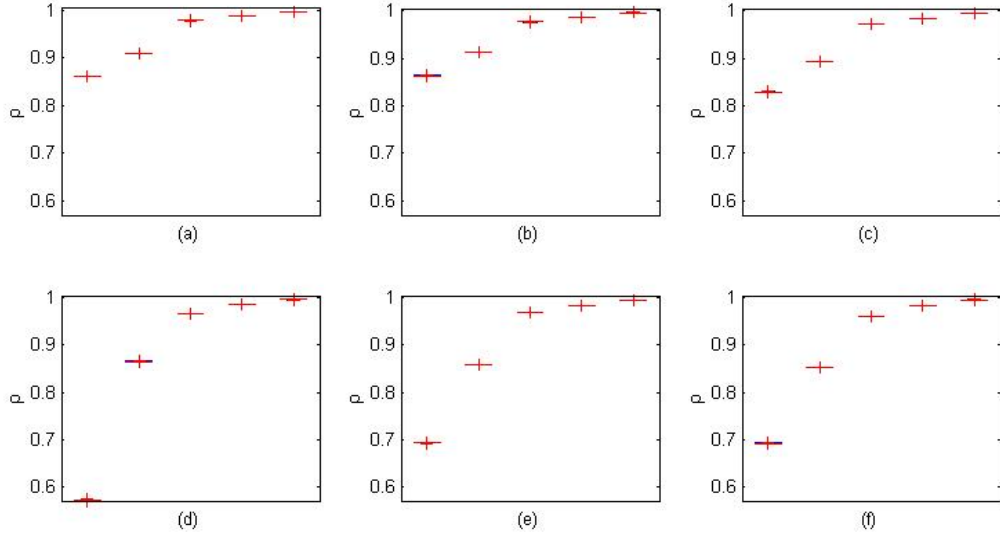


Figure 14: Box-Plots for $\hat{\rho}$. Doppler function, $\rho = 0.9999$, SNR = 7. 1000 replications. 50 initial values randomly chosen from $U(-1, 1)$. Panels: (a) Linear functional step and 'db3'; (b) Linear functional step and 'db6'; (c) Linear functional step and 'sym8'; (d) Nonlinear functional step and 'db3'; (e) Nonlinear functional step and 'db6'; (f) Nonlinear functional step and 'sym8'. In each panel box-plots for sample sizes $n = 512; 1024; 2048; 4096; 8192$ are shown from left to right.

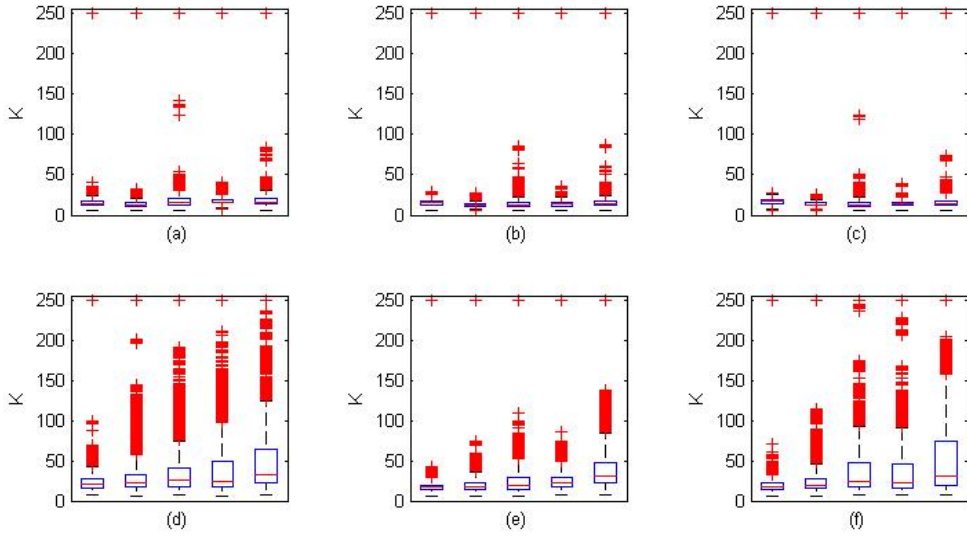


Figure 15: Box-Plots for the number of iterations until numerical convergence. Doppler function, $\rho = 0.99$, SNR = 1. 1000 replications. 50 initial values randomly chosen from $U(-1, 1)$. Panels: (a) Linear functional step and 'db3'; (b) Linear functional step and 'db6'; (c) Linear functional step and 'sym8'; (d) Nonlinear functional step and 'db3'; (e) Nonlinear functional step and 'db6'; (f) Nonlinear functional step and 'sym8'. In each panel box-plots for sample sizes $n = 512; 1024; 2048; 4096; 8192$ are shown from left to right.

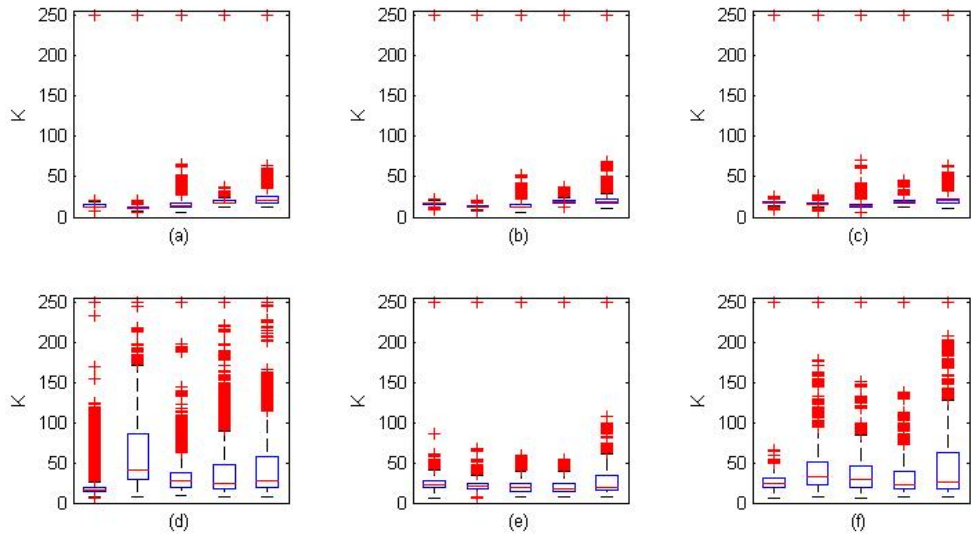


Figure 16: Box-Plots for the number of iterations until numerical convergence. Doppler function, $\rho = 0.99$, $\text{SNR} = 3$. 1000 replications. 50 initial values randomly chosen from $U(-1, 1)$. Panels: (a) Linear functional step and 'db3'; (b) Linear functional step and 'db6'; (c) Linear functional step and 'sym8'; (d) Nonlinear functional step and 'db3'; (e) Nonlinear functional step and 'db6'; (f) Nonlinear functional step and 'sym8'. In each panel box-plots for sample sizes $n = 512; 1024; 2048; 4096; 8192$ are shown from left to right.

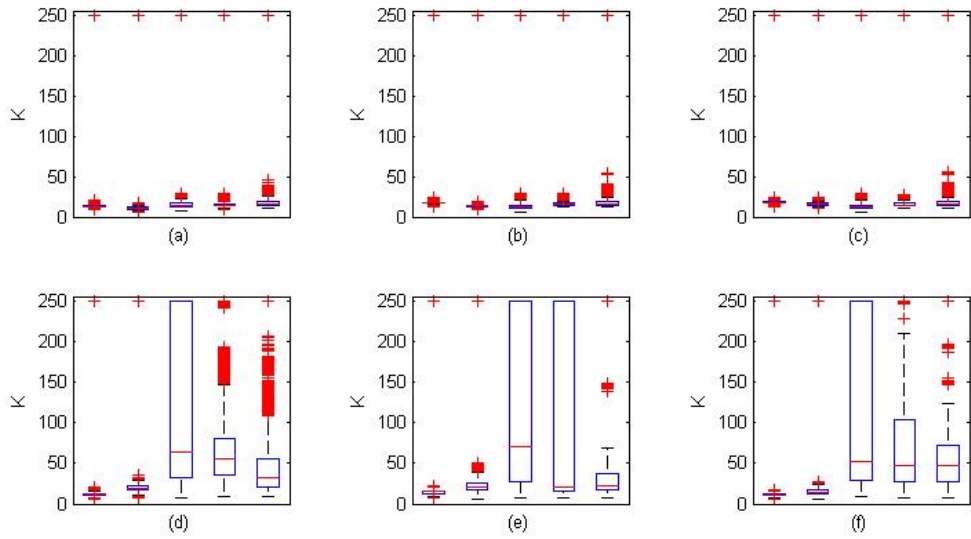


Figure 17: Box-Plots for for the number of iterations until numerical convergence. Doppler function, $\rho = 0.99$, $\text{SNR} = 7$. 1000 replications. 50 initial values randomly chosen from $U(-1, 1)$. Panels: (a) Linear functional step and 'db3'; (b) Linear functional step and 'db6'; (c) Linear functional step and 'sym8'; (d) Nonlinear functional step and 'db3'; (e) Nonlinear functional step and 'db6'; (f) Nonlinear functional step and 'sym8'. In each panel box-plots for sample sizes $n = 512; 1024; 2048; 4096; 8192$ are shown from left to right.

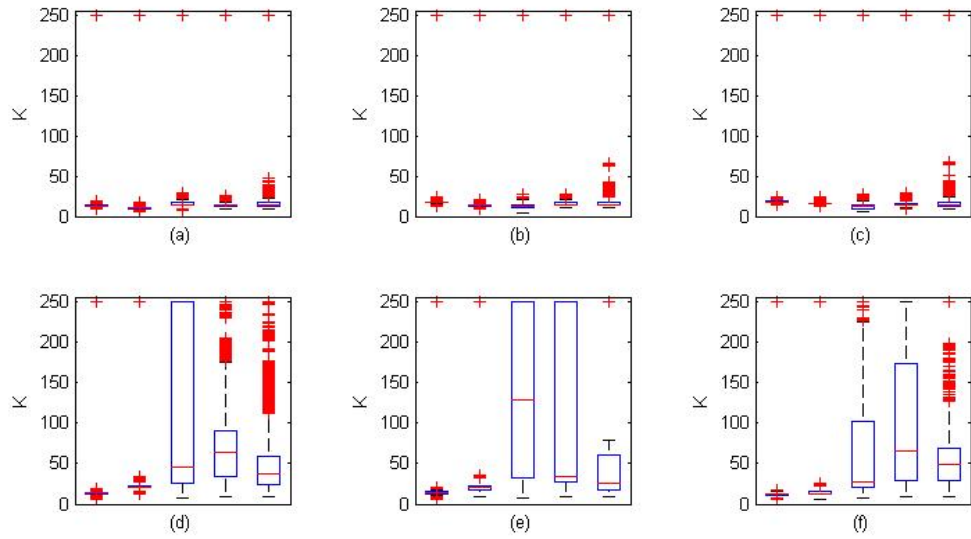


Figure 18: Box-Plots for the number of iterations until numerical convergence. Doppler function, $\rho = 0.9999$, $\text{SNR} = 1$. 1000 replications. 50 initial values randomly chosen from $U(-1, 1)$. Panels: (a) Linear functional step and 'db3'; (b) Linear functional step and 'db6'; (c) Linear functional step and 'sym8'; (d) Nonlinear functional step and 'db3'; (e) Nonlinear functional step and 'db6'; (f) Nonlinear functional step and 'sym8'. In each panel box-plots for sample sizes $n = 512; 1024; 2048; 4096; 8192$ are shown from left to right.

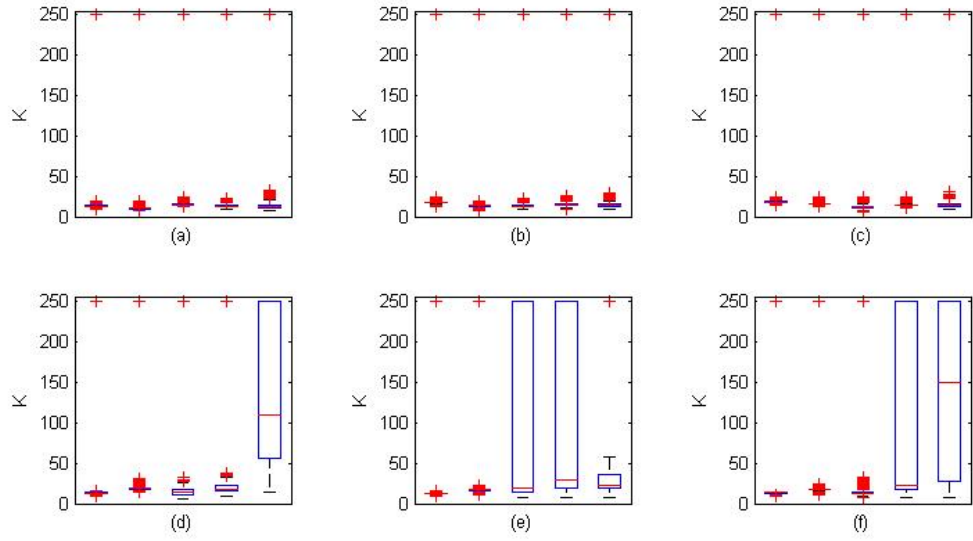


Figure 19: Box-Plots for the number of iterations until numerical convergence. Doppler function, $\rho = 0.9999$, SNR = 3. 1000 replications. 50 initial values randomly chosen from $U(-1, 1)$. Panels: (a) Linear functional step and 'db3'; (b) Linear functional step and 'db6'; (c) Linear functional step and 'sym8'; (d) Nonlinear functional step and 'db3'; (e) Nonlinear functional step and 'db6'; (f) Nonlinear functional step and 'sym8'. In each panel box-plots for sample sizes $n = 512; 1024; 2048; 4096; 8192$ are shown from left to right.

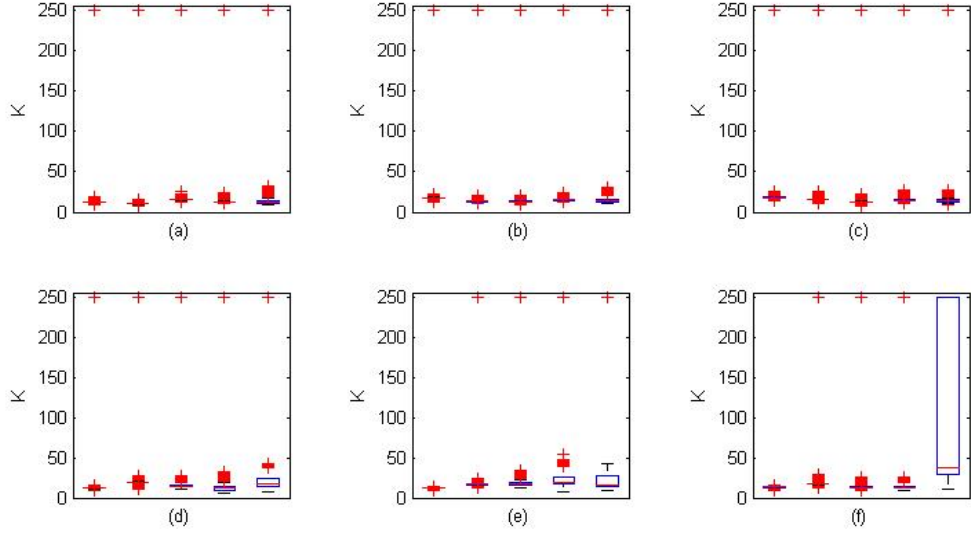


Figure 20: Box-Plots for for the number of iterations until numerical convergence. Doppler function, $\rho = 0.9999$, SNR = 7. 1000 replications. 50 initial values randomly chosen from $U(-1, 1)$. Panels: (a) Linear functional step and 'db3'; (b) Linear functional step and 'db6'; (c) Linear functional step and 'sym8'; (d) Nonlinear functional step and 'db3'; (e) Nonlinear functional step and 'db6'; (f) Nonlinear functional step and 'sym8'. In each panel box-plots for sample sizes $n = 512; 1024; 2048; 4096; 8192$ are shown from left to right.

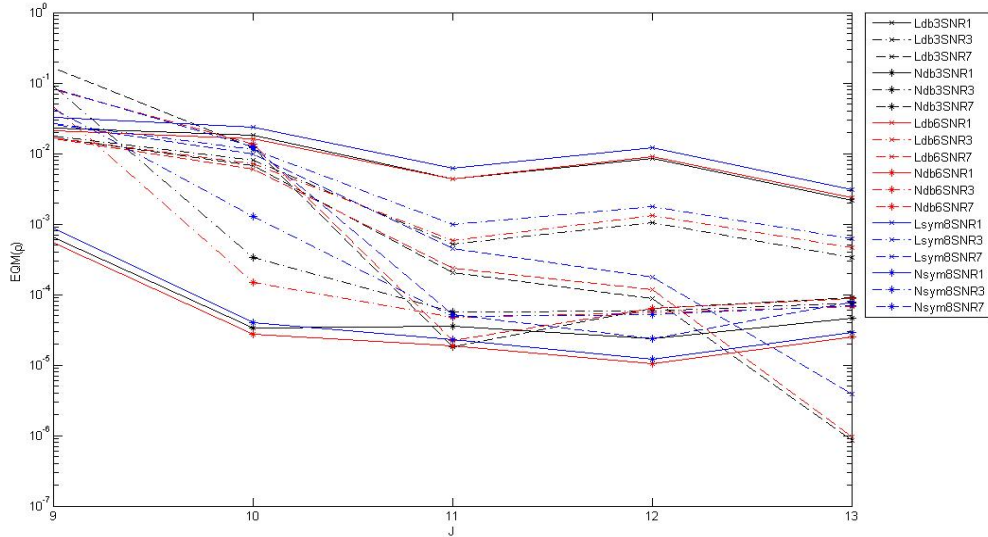


Figure 21: $MSE(\hat{\rho})$ as a function of sample sizes $n = 512; 1024; 2048; 4096; 8192$. Doppler function, $\rho = 0.99$. 1000 replications. 50 initial values randomly chosen from $U(-1, 1)$. 18 plots are labeled by xbasisSNRy , where: $x='L'$ or $'N'$ for linear and nonlinear steps respectively; $\text{basis}='db3', 'db6'$ or $'sym8'$; $y=1,3$ or 7 .

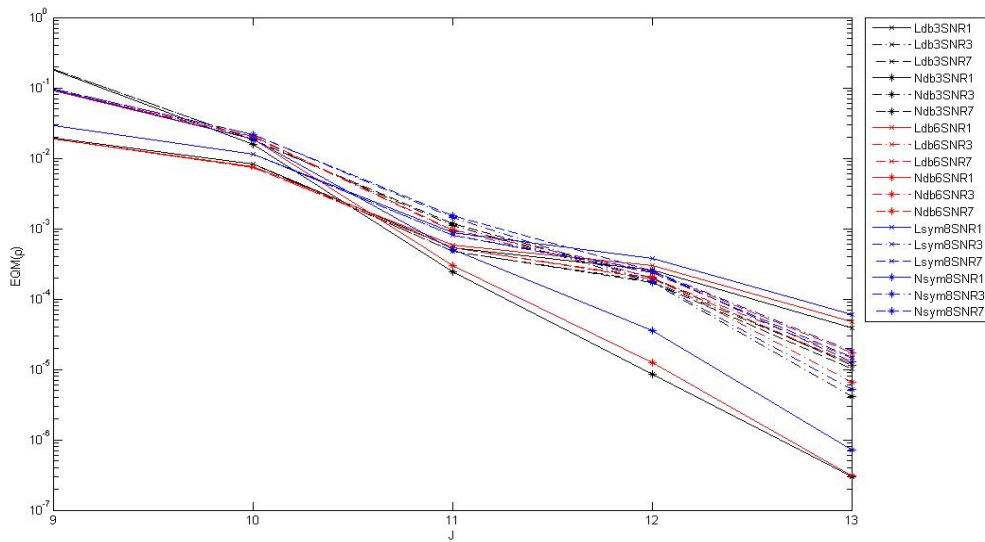


Figure 22: $MSE(\hat{\rho})$ as a function of sample sizes $n = 512; 1024; 2048; 4096; 8192$. Doppler function, $\rho = 0.9999$. 1000 replications. 50 initial values randomly chosen from $U(-1, 1)$. 18 plots are labeled by $x\text{basisSNR}y$, where: $x='L'$ or $'N'$ for linear and nonlinear steps respectively; $\text{basis}='db3'$, $'db6'$ or $'sym8'$; $y=1,3$ or 7 .

Table 5: Integrated Squared Mean Error for \hat{f} . Doppler function, $\rho = 0.99$, SNR = 1, 3, 7. 1000 replications and sample sizes $n = 512; 1024; 2048; 4096; 8192$. 50 initial values randomly chosen from $U(-1, 1)$. Wavelet bases: 'db3', 'db6' and 'sym8'. Functional estimation steps are called 'L', 'NL' or 'NB' if linear, nonlinear with term by term thresholding or nonlinear with block thresholding is employed, respectively. $IMSE(xA)$ represent the average IMSE of \hat{f} for the 1000 replication, 50 initial values in the combination of an SNR= x and thresholding procedure A, where $x=1,3$ or 7 and A='L', 'NL' or 'NB'.

n	SNR=1					SNR=3					SNR=7					
	512	1024	2048	4096	8192	512	1024	2048	4096	8192	512	1024	2048	4096	8192	
db3	$IMSE(1L)$	0.104	0.052	0.026	0.012	0.006	0.155	0.078	0.040	0.015	0.007	0.408	0.205	0.111	0.028	0.014
	$IMSE(2L)$	0.104	0.052	0.026	0.012	0.006	0.155	0.078	0.040	0.015	0.007	0.408	0.205	0.111	0.028	0.014
	$IMSE(3L)$	0.104	0.052	0.026	0.012	0.006	0.155	0.078	0.040	0.015	0.007	0.408	0.205	0.111	0.028	0.014
	$IMSE(1NT)$	0.151	0.138	0.372	0.099	0.225	0.108	0.170	0.748	0.236	0.432	0.118	0.061	0.383	0.540	1.137
	$IMSE(2NT)$	0.151	0.138	0.372	0.099	0.225	0.108	0.170	0.748	0.236	0.432	0.118	0.061	0.382	0.540	1.137
	$IMSE(3NT)$	0.151	0.138	0.372	0.099	0.225	0.109	0.170	0.748	0.236	0.432	0.118	0.061	0.380	0.540	1.137
db6	$IMSE(1NB)$	0.107	0.068	0.089	0.033	0.054	0.094	0.050	0.029	0.025	0.093	0.045	0.027	0.013	0.008	
	$IMSE(2NB)$	0.107	0.068	0.089	0.033	0.054	0.094	0.050	0.029	0.025	0.093	0.045	0.027	0.013	0.008	
	$IMSE(3NB)$	0.107	0.068	0.089	0.033	0.054	0.094	0.050	0.029	0.023	0.025	0.093	0.045	0.027	0.013	
	$IMSE(1L)$	0.103	0.050	0.024	0.011	0.005	0.167	0.078	0.038	0.014	0.006	0.483	0.217	0.107	0.026	0.013
	$IMSE(2L)$	0.103	0.050	0.024	0.011	0.005	0.167	0.078	0.038	0.014	0.006	0.483	0.217	0.107	0.026	0.013
	$IMSE(3L)$	0.103	0.050	0.024	0.011	0.005	0.167	0.078	0.038	0.014	0.006	0.483	0.217	0.107	0.026	0.013
sym8	$IMSE(1NT)$	0.151	0.078	0.065	0.017	0.018	0.119	0.296	0.248	0.077	0.051	0.131	0.058	0.375	0.191	0.184
	$IMSE(2NT)$	0.151	0.078	0.065	0.017	0.018	0.119	0.296	0.248	0.077	0.051	0.131	0.058	0.380	0.192	0.184
	$IMSE(3NT)$	0.151	0.078	0.065	0.017	0.018	0.121	0.297	0.248	0.077	0.051	0.131	0.058	0.385	0.193	0.184
	$IMSE(1NB)$	0.103	0.059	0.048	0.023	0.021	0.093	0.050	0.084	0.082	0.066	0.093	0.045	0.024	0.011	0.072
	$IMSE(2NB)$	0.103	0.059	0.048	0.023	0.021	0.093	0.050	0.084	0.082	0.066	0.093	0.045	0.024	0.011	0.072
	$IMSE(3NB)$	0.103	0.059	0.048	0.023	0.021	0.093	0.050	0.084	0.082	0.066	0.093	0.045	0.024	0.011	0.072
sym8	$IMSE(1L)$	0.101	0.050	0.024	0.012	0.005	0.148	0.072	0.035	0.014	0.006	0.381	0.178	0.089	0.024	0.012
	$IMSE(2L)$	0.101	0.050	0.024	0.012	0.005	0.148	0.072	0.035	0.014	0.006	0.381	0.178	0.089	0.024	0.012
	$IMSE(3L)$	0.101	0.050	0.024	0.012	0.005	0.148	0.072	0.035	0.014	0.006	0.381	0.178	0.089	0.024	0.012
	$IMSE(1NT)$	0.139	0.072	0.116	0.022	0.065	0.116	0.080	0.304	0.080	0.133	0.131	0.062	0.465	0.086	0.483
	$IMSE(2NT)$	0.139	0.072	0.116	0.022	0.065	0.116	0.080	0.304	0.080	0.133	0.131	0.062	0.465	0.086	0.483
	$IMSE(3NT)$	0.139	0.072	0.116	0.022	0.065	0.116	0.080	0.304	0.080	0.133	0.131	0.062	0.465	0.086	0.483
sym8	$IMSE(1NB)$	0.104	0.060	0.091	0.025	0.029	0.093	0.044	0.067	0.073	0.076	0.093	0.044	0.041	0.022	0.099
	$IMSE(2NB)$	0.104	0.060	0.091	0.025	0.029	0.093	0.044	0.067	0.073	0.076	0.093	0.044	0.041	0.022	0.099
	$IMSE(3NB)$	0.104	0.060	0.091	0.025	0.029	0.093	0.044	0.067	0.073	0.076	0.093	0.044	0.040	0.022	0.099

Table 6: Integrated Squared Mean Error for \hat{f} . Doppler function, $\rho = 0.9999$, SNR = 1, 3, 7. 1000 replications and sample sizes $n = 512, 1024, 2048, 4096, 8192$. 50 initial values randomly chosen from $U(-1, 1)$. Wavelet bases: 'db3', 'db6' and 'sym8'. Functional estimation steps are called 'L', 'NL' or 'NB' if linear, nonlinear with term by term thresholding or nonlinear with block thresholding is employed, respectively. $IMSE(xA)$ represent the average $IMSE$ of \hat{f} for the 1000 replication, 50 initial values in the combination of an SNR= x and thresholding procedure A, where $x=1, 3$ or 7 and A= 'L', 'NL' or 'NB'.

n	SNR=1					SNR=3					SNR=7					
	512	1024	2048	4096	8192	512	1024	2048	4096	8192	512	1024	2048	4096	8192	
db3	IMSE(1L)	14.929	7.644	3.727	1.683	0.734	19.993	10.231	5.101	1.938	0.857	45.020	23.056	12.186	3.216	1.530
	IMSE(2L)	14.929	7.644	3.727	1.683	0.734	19.993	10.231	5.101	1.938	0.857	45.020	23.056	12.186	3.216	1.530
	IMSE(3L)	14.929	7.644	3.727	1.683	0.734	19.993	10.231	5.101	1.938	0.857	45.020	23.056	12.186	3.216	1.530
	IMSE(1NT)	14.349	7.339	3.753	1.870	1.705	14.633	7.359	3.556	1.668	0.811	15.680	7.405	3.471	1.631	0.755
	IMSE(2NT)	14.349	7.339	3.753	1.870	1.705	14.633	7.359	3.556	1.668	0.811	15.680	7.405	3.471	1.631	0.755
	IMSE(3NT)	14.349	7.339	3.753	1.870	1.705	14.633	7.359	3.556	1.668	0.811	15.680	7.405	3.471	1.631	0.755
db6	IMSE(1NB)	14.303	7.316	3.556	1.652	0.718	14.313	7.305	3.507	1.642	0.710	13.988	7.154	3.441	1.597	0.713
	IMSE(2NB)	14.303	7.316	3.556	1.652	0.718	14.313	7.305	3.507	1.642	0.710	13.988	7.154	3.441	1.597	0.713
	IMSE(3NB)	14.303	7.316	3.556	1.652	0.718	14.313	7.305	3.507	1.642	0.710	13.988	7.154	3.441	1.597	0.713
	IMSE(1L)	15.078	7.671	3.721	1.679	0.730	21.382	10.488	5.049	1.917	0.841	52.649	24.468	11.914	3.120	1.460
	IMSE(2L)	15.078	7.671	3.721	1.679	0.730	21.382	10.488	5.049	1.917	0.841	52.649	24.468	11.914	3.120	1.460
	IMSE(3L)	15.078	7.671	3.721	1.679	0.730	21.382	10.488	5.049	1.917	0.841	52.649	24.468	11.914	3.120	1.460
sym8	IMSE(1NT)	14.366	7.326	3.700	1.793	0.910	14.849	7.337	3.548	1.681	0.797	16.904	7.273	3.475	1.634	0.737
	IMSE(2NT)	14.366	7.326	3.700	1.793	0.910	14.849	7.337	3.548	1.681	0.797	16.904	7.273	3.475	1.634	0.737
	IMSE(3NT)	14.366	7.326	3.701	1.793	0.910	14.849	7.337	3.548	1.681	0.797	16.904	7.273	3.475	1.634	0.737
	IMSE(1NB)	14.302	7.315	3.557	1.650	0.746	14.312	7.305	3.507	1.642	0.708	13.987	7.153	3.441	1.596	0.713
	IMSE(2NB)	14.302	7.315	3.557	1.650	0.746	14.312	7.305	3.507	1.642	0.708	13.987	7.153	3.441	1.596	0.713
	IMSE(3NB)	14.302	7.315	3.557	1.650	0.746	14.312	7.305	3.507	1.642	0.708	13.987	7.153	3.441	1.596	0.713
sym8	IMSE(1L)	14.874	7.591	3.685	1.676	0.729	19.526	9.767	4.717	1.882	0.823	42.498	20.545	10.086	2.922	1.363
	IMSE(2L)	14.874	7.591	3.685	1.676	0.729	19.526	9.767	4.717	1.882	0.823	42.498	20.545	10.086	2.922	1.363
	IMSE(3L)	14.874	7.591	3.685	1.676	0.729	19.526	9.767	4.717	1.882	0.823	42.498	20.545	10.086	2.922	1.363
	IMSE(1NT)	14.365	7.329	3.660	1.798	1.353	14.845	7.332	3.535	1.705	0.794	16.892	7.290	3.461	1.627	0.757
	IMSE(2NT)	14.365	7.329	3.660	1.798	1.353	14.845	7.332	3.535	1.705	0.794	16.892	7.290	3.461	1.627	0.757
	IMSE(3NT)	14.365	7.329	3.660	1.798	1.353	14.845	7.332	3.535	1.705	0.794	16.892	7.290	3.461	1.627	0.757
sym8	IMSE(1NB)	14.302	7.315	3.552	1.673	0.718	14.313	7.304	3.507	1.642	0.708	13.987	7.153	3.441	1.596	0.713
	IMSE(2NB)	14.302	7.315	3.552	1.673	0.718	14.313	7.304	3.507	1.642	0.708	13.987	7.153	3.441	1.596	0.713
	IMSE(3NB)	14.302	7.315	3.552	1.673	0.718	14.313	7.304	3.507	1.642	0.708	13.987	7.153	3.441	1.596	0.713